Absorption of deuterium in palladium rods: model vs. experiment

S. Szpak, P.A. Mosier-Boss and C.J. Gabriel
Naval Command, Control and Ocean Surveillance Center, RDT and E Division, San Diego, CA 92152-5000 (USA)

J.J. Smith
Department of Energy, Washington, DC 20585 (USA)
(Received 19 February 1993; in revised form 6 July 1993)

ABSTRACT

The electrochemical charging of Pd rods by deuterium involves a complex coupling of electrochemical, interfacial and transport processes. In order to predict the overpotential, surface coverage and bulk loading of the electrode during charging, a model has been developed that incorporates the essential features of these processes and involves variables such as the electrochemical rate constants, the bulk diffusion coefficient and the charging current. Features of the computed time dependence of the bulk loading are then compared with published experimental charging curves. New microscopic observations and X-ray diffraction data provide further evidence for the details of the charging process.

1. INTRODUCTION

In an earlier paper [1] we presented a model describing the charging of Pd rods by electrochemically generated deuterium. This model, which is based upon the coupling of interfacial processes with the diffusional transport of interstitials, offers certain predictive capabilities with respect to the charging process. In particular, we examined the effect of the magnitude of the rate constants of the electrochemical steps and the charging current on the surface coverage, the electrode potential and the electrode charging. Subsequently, Riley et al. [2] reported on the experimentally observed absorption of deuterium into the Pd lattice of catodically polarized electrodes and presented results with which the predictions of our model are qualitatively in good agreement. We take this agreement as evidence for the general validity of the model and its assumptions and use the results as a basis for a refined interpretation of the charging process.

While our previous discussion of the model [1] was essentially limited to the examination of the behavior of a set of coupled differential equations, this paper presents the comparison of the model and its predictions with experiment using the data of ref. 2. We explore the relationship between the various operating fluxes and the initial charging rate as well as the asymptotic level of the electrode charging. We include new results based upon an examination of microscopic observations and X-ray diffraction data of a charged Pd electrode. Finally, we conclude with a discussion of the strengths and weaknesses of the model in the light of the experimental evidence.

2. INTERPRETATION OF EXPERIMENTAL DATA OF RILEY ET AL.

The data published by Riley et al. [2] show four characteristic features of the D/Pd system during charging: (i) the existence of an apparent threshold value for the cathodic current density (CD) above which the initial charging rate does not increase, implying the existence of a CD-dependent charging mode(s); (ii) an unexpected dependence of the asymptotic electrode loading on the charging CD, i.e., the appearance of a maximum (ref. 2, Fig. 5); (iii) a slower rate for “unloading” than for “loading,” which implies that the rate of transport between the metal electrode and bulk electrolyte, i.e., across

the interphase, depends on the direction—an unlikely situation for diffusion control; (iv) an initial charging rate that depends, for the most part, inversely on the diameter of the Pd electrode.

In their interpretation, by assuming diffusion control, Riley et al. have considered only events occurring in the electrode interior and have disregarded the influence of a non-autonomous interphase on the charging process. In what follows, we discuss their data in the context of our model and offer a somewhat different interpretation from that provided in ref. 2, showing that (i) and (ii) are natural consequences of the model while (iii) and possibly (iv) require the presence of more complex mechanisms.

In the interpretation of the charging data of ref. 2, it is convenient to introduce the concept of the charging efficiency for a cylindrical electrode of radius r, defined here as the ratio of the absorbed deuterium to that which is generated by electrolysis at a current density j within a time interval Δt and given by

$$\epsilon = \frac{Z_m F}{2} \frac{r}{j} \frac{\Delta Q}{\Delta t} \tag{1}$$

where Z_m is the maximum number of available sites per unit volume, F is the Faraday constant and ΔQ is the corresponding change in the loading ratio Q of deuterium to palladium, conveniently expressed in terms of the D/Pd atomic ratio since Z_m is taken here to be the number density of Pd. The first factor on the right-hand side in eqn. (1) is a constant (equal to 5.45×10^3 C cm^{-3} for a Pd electrode) independent of the manner in which the experiment is carried out; the second factor is controlled by the investigator. The third factor is the measured charging rate and reflects the time dependence of the charging efficiency ε for an experiment. The initial charging efficiency characterizes the interphase processes independently of the electrode geometry, so that the initial charging rate varies with r as $1/r$. This relationship is independent of the details of the model.

The processes associated with the electrolytic charging of the Pd electrode are shown in Fig. 1. As indicated, there are six fluxes in operation, resulting in a large number of governing parameters. Because of the large number of parameters involved, the predicted results are not necessarily computed with the same values of CD or electrode radius as those for which the experiments were done. Rather, a limited number of values are chosen to illustrate possible model behavior, with the idea in mind that a more elaborate procedure for choosing the model parameters could produce a better experimental fit if in fact the model does exhibit the proper behavior.

The model parameters that we have used here are listed in Table 1. Several of the parameters differ from those used earlier in ref. 1 where we provided a qualitative description of Pd/D charging. In this paper, in order to obtain agreement with the experimental data reported in ref. 2, we have chosen model parameters accordingly. Of particular significance are the changes in Γ_m, θ_0 and ξ_0. The surface density of sites, Γm, was taken to be 0.005 of the maximum number of surface sites consistent with our choice of Zm. The initial values of surface coverage and bulk loading, θ_0 and ξ_0, were chosen to be consistent with the observation of Riley et al. [2] that the equilibrated loading is essentially zero.

2.1. Threshold CD; Charging Efficiency; Asymptotic Charging Level

Using the parameters in Table 1 and the diffusion coefficient for β-PdD, the results of model calculations for a cylindrical electrode of radius 0.05 cm charged at current densities ranging from 30 to 240 mA cm^{-2} are shown in Figs. 2 and 3. It is seen that the calculated charging curves reproduce well the experimental data reported in ref. 2, Fig 5. In particular, Fig. 2 is a family of charging curves as a

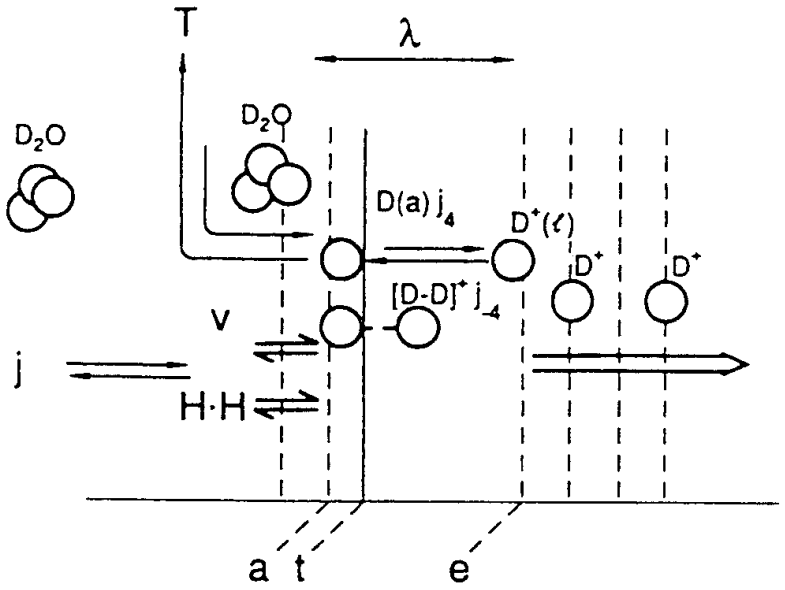

Figure 1. Concept of the Pd/D_2O interphase [1,5,7]: a, adsorption layer; t, charge transfer layer; e, surface dividing the interphase and the bulk electrode; l, lattice; j, total current; H.H., Heyrovsky-Horiuti path; T, Tafel path; V, Volmer path: j_4 and j_{-4}, adsorbed–adsorbed exchange; l, non-autonomous interphase region.

Table 1. Input data for model calculation (cf ref. 9).

Parameter	Value
$[D_2O]$	5.5×10^{-2} mol cm^{-3}
$[OD^-]$	1.0×10^{-4} mol cm^{-3}
$[D_2(s)]$	8.3×10^{-7} mol cm^{-3}
k_1	1000 cm^3 mol^{-1} s^{-1}
k_2	100 cm^3 mol^{-1} s^{-1}
k_3	1000 cm^2 mol^{-1} s^{-1}
k_4	1.0×10^7 cm^3 mol^{-1} s^{-1}
Z_m	0.113 mol cm^{-3}
Γ_m	1.4×10^{-11} mol cm^{-2}
C	4.0×10^{-3} F cm^{-2}
α	0.5
β	0.3
θ_0	1.0×10^{-5}
ζ_0	5.0×10^{-5}
N	10

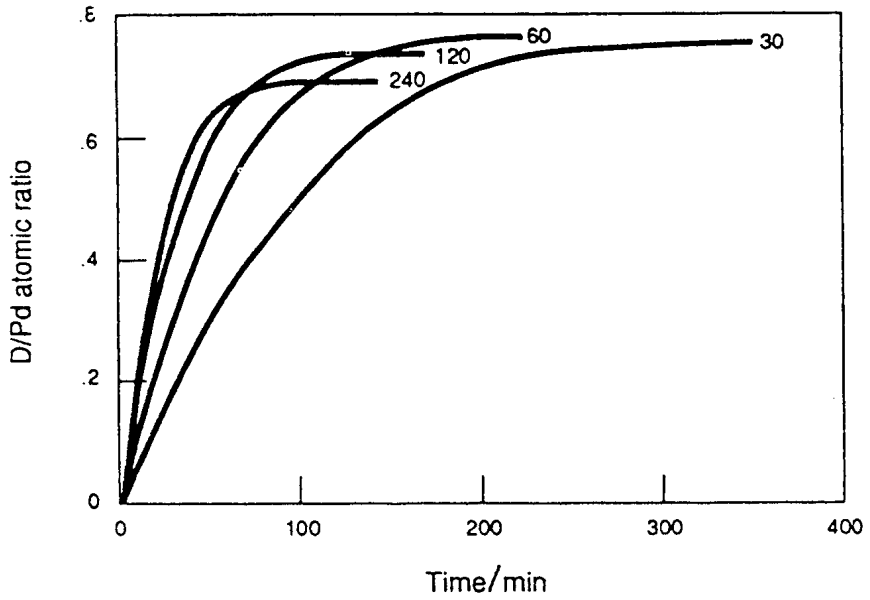

Figure 2. Model calculation of loading curves as a function of current density: electrode radius 0.05 cm; current densities are indicated in mA cm^{-2}; diffusion coefficient 1.6×10^{-6} cm^2 s^{-1}, other parameters are listed in Table 1.

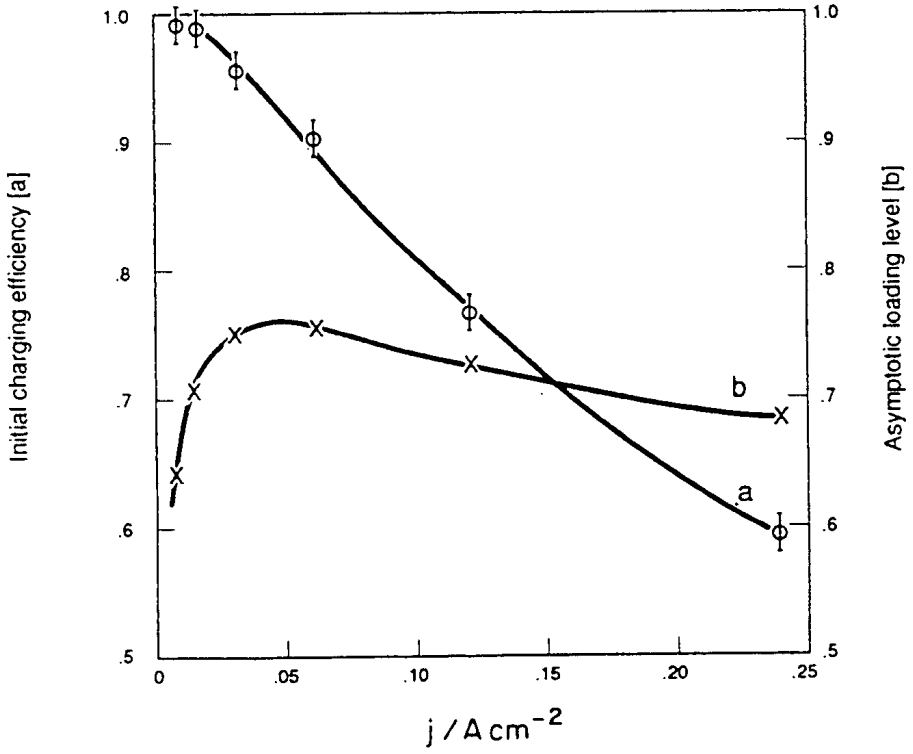

Figure 3. Model calculations as a function of current density: a, initial charging efficiency; b, asymptotic loading level; electrode radius 0.05 cm; diffusion coefficient 1.6×10^{-6} cm^2 s^{-1}; other parameters are listed in Table 1.

function of CD and illustrates that the model predicts a saturation of the initial charging rate. Figure 3, curve A plots the initial charging efficiency calculated by eqn. (1) and Fig. 3, curve B the asymptotic loading level obtained from the curves of Fig. 2. The model predicts a brief period of rapidly varying

charging rate, depending on the electrode capacitance, which would not be observable experimentally, therefore the initial charging rates used in eqn. (1) were obtained graphically from expanded versions of the data shown in Fig. 2 and consequently contain a measurement error. In terms of the model, what has been referred to in ref. 2 as a threshold effect in the charging rate wit increasing CD may in reality be a saturation of the charging rate caused by a decrease in the effectiveness of the Volmer path with respect to the Heyrovsky–Horiuti path for charge transfer, coincidentally resulting in a charging efficiency that appears to be inversely proportional to the current density. Further, the maximum in the measured loading curve asymptotic levels as a function of CD, i.e., characteristic feature (ii) (see Fig. 3 and eqn. (II) of ref. 1), probably results from the same shift in the charge transfer rather than from changes in the Tafel path or the absorption of deuterium, since only the Volmer and Heyrovsky–Horiuti paths (eqn. (I) and (II) of ref. 1 respectively) exhibit a CD (overpotential) dependence.

It is of interest to note that earlier calculations that did not include desorption (the Heyrovsky–Horiuti path) showed an instability in the computed overpotential, suggesting that the shift in balance between adsorption and desorption plays an essential role in the electrode charging. However, a direct computation of the charging currents for the two paths, which we have not done, would be desirable to clarify this behavior.

2.2. Electrode Loading vs. Unloading

Evidence of an active interphase is provided by the difference in the loading and unloading rates and the incomplete unloading which leaves 0.1–0.15 D/Pd remaining, i.e., characteristic feature (iii). This behavior is not consistent with diffusion control. The observed asymmetry between the loading and unloading time dependences would not be predicted by a linear diffusion model. Such a model would be analogous to ordinary diffusion with constant initial bulk concentration, yielding a solution that is the product of a time-dependent factor containing geometrical information, but not initial conditions, and a function of the difference between the initial bulk concentration and the surface concentration (see e.g. eqn. 2.4.1. of ref. 3, p. 97). Although this asymmetry would be consistent with surface control as predicted by the model if e.g., $k_{-4} \gg k_4$ in eqn. (IV) of ref. 1, this choice does not reproduce well the other characteristic features (i) and (ii) and fails to predict incomplete unloading. Further, this asymmetry cannot be explained by diffusion alone even if $D_\alpha < D_\beta$ by about an order of magnitude [4] because of the required continuity of flux across the $\alpha \rightarrow \beta$ dividing plane. The continuity of flux and the low D/Pd ratio for the α phase would result in a very thin α region that can be identified with the interphase itself. Consequently, another mechanism(s) must be considered in seeking the explanation for this observation. For example, the incomplete unloading at a CD of 60 mA cm^{-2} or larger may be due to blocking of the electrode surface by an oxide layer in as much as the applied current would exceed the diffusion current associated with the transport of absorbed deuterium out of the Pd lattice.

Evidently there exists a mechanism(s) that causes the absorbed deuteirum to affect the loading and unloading rates differently. If we assign an active role to the interphase as suggested by the surface morphology (see the subsequent discussion of the interphase), then a mechanism is provided. To illustrate this, the electro-chemical potential of the adsorbed deuterium contains a contribution resulting from the electrode overpotential while that in the bulk is affected by contributions involving the electronic as well as mechanical interactions. Upon current reversal (during unloading) the magnitude of the driving force may be different and the asymmetry would follow naturally.

2.3. Effect of Electrode Radius

The effect of the electrode radius on the calculated charging curves is shown in Fig. 4, where the diffusion coefficient for β-PdD was used. It illustrates agreement with the experimental data (see ref. 2, Fig. 6) except for the electrode with a radius of 0.1 cm. The anomaly in the latter concerns the initial portions of the measured charging curves for which there is no observed difference in slope between the data for radii of 0.05 and 0.1 cm, requiring that the initial charging efficiency be proportional to the electrode radius—an unrealistic condition. Otherwise, eqn. (1), which predicts the slopws of the charging curves to have a $1/r$ dependence initially, is well satisfied. All three calculated curves exhibit an initial charging efficiency of 0.78, whereas the measured curves of ref. 2, Fig. 6 show an initial charging efficiency of about 0.8 for the 0.05 and 0.2 cm radii data and a unrealistically high value of about 1.6 for the 0.1 cm radius data. Because the reduction rates have no dependence of the asymptotic charging level on the radius of the electrode and apparently none is observed.

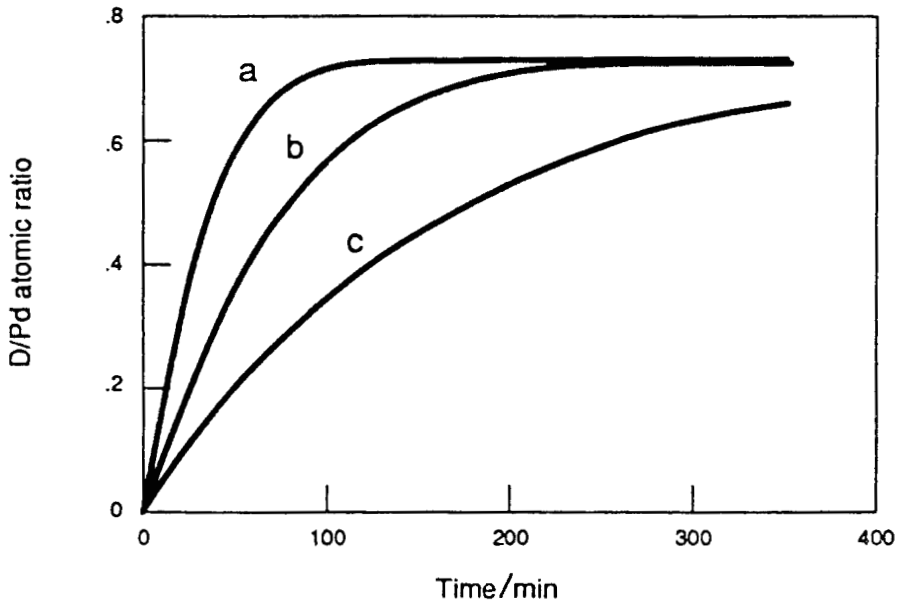

Figure 4. Model calculation of loading curves as a function of electrode radius: a, 0.05 cm; b, 0.1 cm; c, 0.2 cm; current density 120 mA cm^{-2}; diffusion coefficient 1.6×10^{-6} cm^2 s^{-1}; other parameters are listed in Table 1.

2.4. Electrode-Loading Mode

Participation of the interphase in the course of the electrode charging can be examined numerically by changing the value of the diffusion coefficient used in the model computations. As the diffusion coefficient is made smaller, a shift to transport control must occur. The effect of varying the diffusion coefficient on the charging curves is illustrated in Fig. 5. At the highest CD a significant change is noted in the shape of the charging curve for the diffusion coefficient of 1.6×10^{-7} cm^2 s^{-1}. In contrast, at the lower CDs only a small change is achieved for the same changes in the diffusion coefficient, indicating a relative increase in surface control at lower CD as expected. This further indicates that a transition between diffusion and surface control occurs within the practical range of current densities at the diffusion coefficient operable in the system. A comparison with Fig. 5 of ref. 2 suggests that the observed charging rates were limited by diffusion at CDs of 60 mA cm^{-2} and greater, while for lower CDs the limitation may have been the surface reactions.

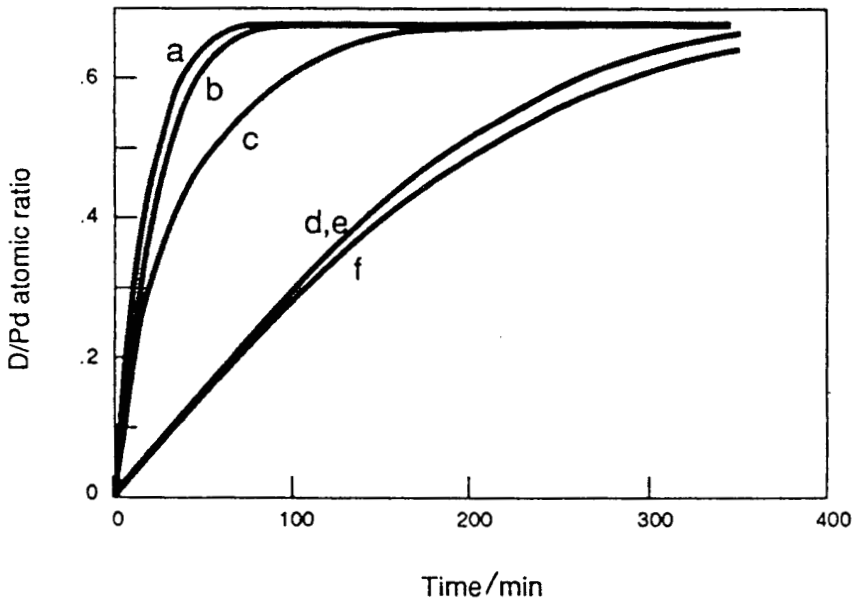

Figure 5. Model calculation of loading curves for current densities *j*/mA cm^{-2} and diffusion coefficients D/cm^2 s^{-1}: a, *j* = 240, D = 1.6 × 10^{-5}; b, *j* = 240, D = 1.6 × 10^{-6}; c, *j* = 240, D = 1.6 × 10^{-7}; d, *j* = 15, D = 1.6 × 10^{-5}; e, *j* = 15, D = 1.6 × 10^{-6}; f, *j* = 15, D = 1.6 × 10^{-7}; electrode radius 0.05 cm; other parameters are listed in Table 1.

Figure 5 also indicates that a more realistic treatment of the bulk diffusion to include differences in diffusion coefficients for α- and β-PdD would not predict significantly different charging curves except at higher CDs, where there is diffusion control of the charging process.

3. EVOLUTION OF THE PDD/D_2O INTERPHASE

The surface inhomogeneity with regard to the absorption of hydrogen isotopes and the composition of the interphase, as revealed by X–ray diffraction spectroscopy, provide further evidence for the active participation of the interphase in the course of charging–discharging processes. The experimentally observed difference in the loading and unloading rates and the presence of residual deuterium in the Pd electrode suggest that other processes, beyond those contained in the model, play a significant role.

3.1. Surface Inhomogeneity

The active participations of the Pd surface manifests itself as inhomogeneous changes in the surface morphology of Pd electrodes during their prolonged exposure to evolving hydrogen and deuterium as reported by Rolison et al. [5]. Another way to demonstrate the inhomogeneity of a Pd surface, particularly with regard to absorption, is to view it using Nomarski optics [6] so that regions of preferred absorption can be differentiated. An example of the experimental arrangement is illustrated in Fig. 6. A Pd wire, heat treated at the recrystallization temperature to ensure large grains, was mounted in an epoxy resin, polished (diamond paste on silk followed by a light polish with 0.05 m Al_2O_3 on microcloth) and etched (anodic etch in 50% HCl). A hole was drilled through which a Pt counterelectrode was inserted and the cell was closed with a thin Mylar film. The so–constructed cell was connected to a power source and placed in a metallograph (Leco Neophot 21) equipped with Nomarski optics. Images of the electrode surface were continuously recorded on videotape. The observed changes within a single grain, which is outlined, are illustrated in Fig. 7. It is unlikely that

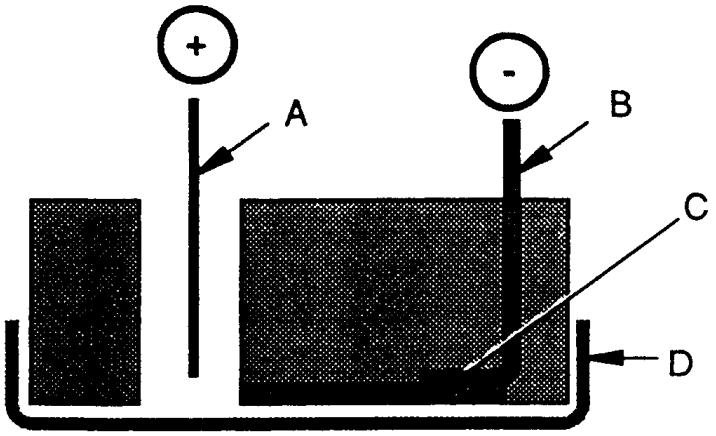

Figure 6. Electrolytic cell for examination of an electrode surface by Nomarski optics: A, Pt counterelectrode; B, Cu wire spot welded to a Pd electrode; C, etched Pd surface; D, Mylar film.

Figure 7. Preferred locations of D_2 penetration into a single Pd grain as obtained by electronic subtraction of Nomarski images. After cathodically charging the Pd electrode at 5 mA for 30 min, an image was recorded. This image was digitized and the image of the grain at rest potential was subtracted out. The subtracted image is shown with the individual grain outlined. The magnification of the microscope is X 400.

the changes observed in the grain can be attributed to the surface or near–surface cracking that has been found after long charging times at high current densities [7]. Rather, these changes are attributed to localized volume extension and indicate that even within a single grain there are preferred sites of absorption—a conclusion also reached by Rolison et al. [5].

3.2. Supercharged Region

The present model employs a simple, passive interphase. In actuality, as indicated by Bucur and Bota [8], the H atoms accumulate in the interphase, i.e. a supercharged region exists. To explore

further the Pd/D_20 interphase, we examined the time evolution of the in situ X–ray spectra covering a rather narrow 2θ range from 35° to 55°. For this purpose a cell, shown in Fig. 8, connected to a potentiostat (PAR model 363) was placed in an X–ray diffraction system (Rigaku RU 200 H). The cell body and stem, on to which a Pd foil (Cu clad on one side to ensure containment of the deuterium) was attached, were constructed out of a chemically inert material (TPX). The cell was provided with a thin polyethylene window, which minimized scattering of the X–rays, and a small hole in the top of the cell body, which permitted both the escape of gas and the addition of electrolyte as needed. The cell was assembled in a dry box.

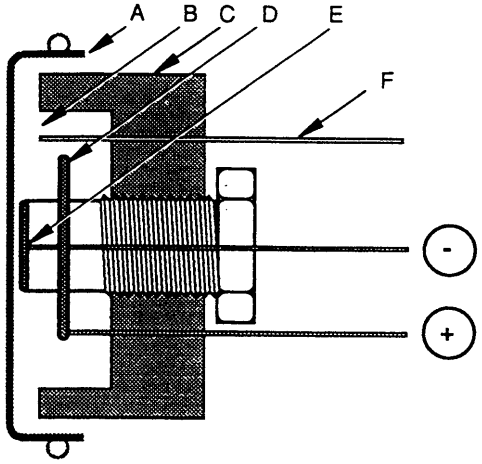

Figure 8. Electrolytic cell for in situ X-ray spectroscopy; A, polyethylene window; B, electrolyte cavity; C, cell body (TPX); D, Pt counterelectrode; E, Pd foil; F, Pd reference electrode.

Figure 9 shows the diffraction spectra for the Pd foil at rest potential (spectrum A) and at subsequent times and potentials (spectra B—E). At rest potential the polycrystalline Pd foil exhibits two peaks: one at 40.377° and another at 46.924° due to reflections from the 200 and 111 planes respectively. After 2 h of charging at 1.5 V negative overpotential, during which the electrode appearance had not changed, new peaks at 37.758° and 45.025° emerged, indicating formation of the β–PdD phase (spectra B and C). Comparison of the ratios of the 111 peaks to the 200 peaks for the Pd and β–PdD phase leads to the conclusion that deuterium preferentially enters the Pd lattice through the 111 sites. This conclusion agrees well with that based on theoretical calculations [9]. With prolonged charging, the silvery color of metallic palladium changed to black. After 24 h of charging, the recorded spectrum shows only two peaks attributed to the β–PdD phase (spectrum E). The 111 and 200 reflection peaks have shifted to lower values, indicating further expansion of the lattice. With continued charging, these peaks have broadened (spectra D and E) but their peak positions have stayed relatively constant. We interpret both this broadening and the shift to lower 2θ angles as indicating the presence of a supercharged layer.

4. STRENGTHS AND WEAKNESSES OF THE MODEL

Models are used both to simulate a complex reality by simpler arrangements and to display the essential features of a physical system. Often even a simplified model clarifies the interpretation of ambiguous data and avoids lengthy calculations that might be irrelevant to the problem considered. In the present case even our simple model indicates that the observed charging behavior of Pd electrodes cannot be explained solely by the diffusion characteristics of deuterium in the bulk but must include consideration of the surface reactions as well. This is especially true at lower CDs.

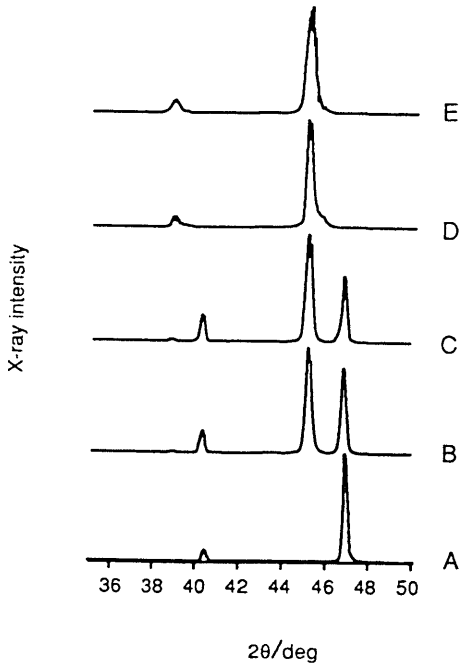

Figure 9. Progress in electrode loading by X-ray spectra: A, metallic Pd; B and C, transition from metallic to β-PdD phase; D and E, β-PdD phase (see text for overpotentials and charging times).

We have applied a model where the structure of the interphase as well as the operating driving forces are determined by participating processes occurring in both contacting phases. However, we have treated the interphase as a passive element, i.e. in effect assuming that the surface is homogeneous with respect to the chemical potential. Such an assumption is not realistic (see Fig. 7), although it might be justified on the basis of the existence of the supercharged region. Clearly an assumption of uniform surface coverage of the Pd rod cannot be made. Even so, the model does remarkably well in predicting a saturation of the initial charging rate and a non–monotonic dependence of the asymptotic charging level on CD. The time required to obtain a full charge is also predictable with reasonable model parameters. This model provides a framework within which questions such as the relative influence of the Volmer and Heyrovsky—Horiuti charge transfer paths as a function of CD can be considered.

Although the model does predict some small asymmetry in loading and unloading, it does not appear able to predict as large an effect as was observed and it does not predict the incomplete electrode unloading at all. Evidently, a more realistic model should incorporate an active interphase that will provide mechanisms for asymmetric loading and also explain why the charging rate and level can differ from electrode to electrode.

ACKNOWLEDGMENT

The authors thank Dr. F. Gordon for his enthusiastic support of this project.

REFERENCES

1. S. Szpak, C.J. Gabriel, J.J. Smith and R.J. Nowak, J. Electroanal. Chem., 309(1991)273.

2. A.M. Riley, J.D. Seader, D.W. Pershing and *C.* Walling, J. Electrochem. Soc., 139(1992)1342.

3. J.D. Fast, Interaction of Metals and Gases, Vol. II, Barnes and Noble, New York, 1971.

4. M. V. Stackelberg and P. Ludwig, Z. Naturf. A, 19 (1964)93.

5. D. Rolison, W.E. O'Grady, R.J. Doyle and P.P. Trzaskoma, Anomalies in the surface analysis of deuterated palladium, Proc. First Ann. Conf. on Cold Fusion, Salt Lake City, UT, 1990 p. 272.

6. W. Lang, Nomarski Differential Interference–contrast microscopy, Zeiss Informations, Oberkochen, 1968.

7. S. Gurswamy and M.E. Wadsworth, Metallurgical aspects in cold fusion experiments, Proc. First Ann. Conf. on Cold Fusion, Salt Lake City, UT, 1990 p. 314.

8. R.V. Bucur and F. Bota, Electrochim. Acta, 29(1984)103. 9 H.–G. Fritsche, Z. Naturf. A, 38 (1983)1118.